

WOJCIECH GRZEGORZEK*, STANISŁAW ŚCIESZKA*

Prediction on friction characteristics of mine hoist disc brakes using artificial neural networks

Key words

Mine hoist disc brakes, prediction on friction characteristics, coefficient of friction, neural networks.

Słowa kluczowe

Hamulce maszyn wyciągowych, prognozowanie charakterystyk ciernych, współczynnik tarcia, sieci neuronowe.

Summary

Safety and reliability are the main requirements for brake devices in the mining winding installations. Trouble-free performance under changing braking parameters is mandatory. Therefore, selection of the right materials for the friction brake elements (pads and discs) is the most challenging task for brake system designers. The coefficient of friction for the friction couple should be relatively high (≈ 0.4); but, above all, it should be stable. In order to achieve the desired brake friction couple performance, a new approach to the prediction of the tribological processes versus friction materials formulation is needed. The paper shows that the application of the artificial neural network (ANN) can be productive in modelling complex, multi-dimensional functional relationships directly from experimental data. The ANN can learn to produce an input/output relationship, and the model of friction brake behaviour can be established.

* Silesian University of Technology, Faculty of Mining and Geology, Institute of Mining Mechanisation, Akademicka 2A Street, 44-100 Gliwice, Poland; wojciech.grzegorzek@polsl.pl, stanislaw.scieszka@polsl.pl.

Introduction

Mine hoist brake systems have several distinctive design features and specific operational requirements, which make them differ from an automotive brakes and even other industrial brake systems. Winders installed in mines are designed to raise and lower, in fully controlled manner, the mass in excess of 40 Mg in a mine shaft over one kilometre deep. Instead of the ϕ 300 mm size typical for automotive disc brake, there might be, e.g., 16 brake callipers acting on two approximately 6 metre diameter discs connected to the drum (Fig. 1) able to stop the payload moving at a speed of up to 20 m/s (Table 1) [1, 2].

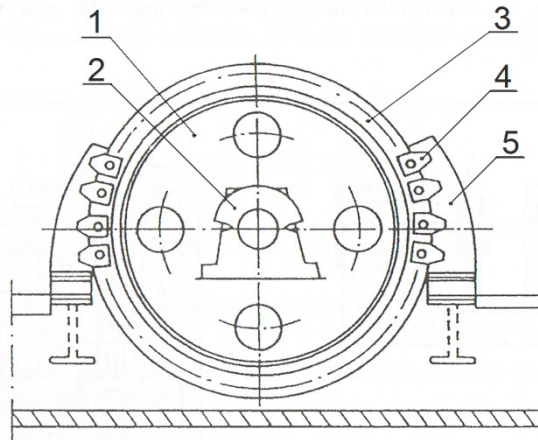


Fig. 1. Multi-rope friction sheaf hoist with hydraulic disc brake system, where: 1 – multi-rope drum, 2 – journal bearing, 3 – brake disc connected to the drum, 4 – hydraulic brake calliper, 5 – callipers stand

Rys. 1. Wielolinowa maszyna wyciągowa z hydraulicznym hamulcem tarczowym, gdzie: 1 – bęben wielolinowy, 2 – łożysko, 3 – tarcza hamulca, 4 – hydrauliczne szczękowe zespoły robocze, 5 – stojak

Table 1. Mine host brake's design and operational parameters [2]
Tabela 1. Parametry konstrukcyjne i użytkowe hamulców maszyn wyciągowych [2]

No	Parameter	Operating range	Dimension
1	Initial sliding speed, v	10 – 20	m/s
2	Normal pressure, p	0.9 – 1.5	MPa
3	Maximal friction energy density, ρ_t	55 – 240	kW/m ²
4	Brake disc's surface temperature, T	60 – 380	°C
5	Duration of braking, t_h	6 – 17	s
6	Friction surface, A_t	0.12 – 0.48	m ²
7	Radius of friction, R_t	2.20 – 3.11	m
8	Friction torque, M_t	0.9 – 2.8	MNm

To stop the dram (together with ropes, skips and payload), friction materials in the form of brake pads mounted in the brake callipers (Fig. 1) are forced hydraulically against both sides of the disc. Friction causes the discs and attached moving parts of the winder to stop. The friction energy is converted into heat during retardation, which, in consequence, means temperature elevation on the friction surfaces of brake pads and discs. The extreme tribological loading on the friction brake elements take place during emergency braking, which can be initiated at full speed by the power lost, a control malfunction, or faulty operation.

The emergency braking must be done with control giving a constant predetermined retardation independent of the braking condition. The above design features and operational requirements are particularly challenging for the friction pads material, because it should maintain a stable coefficient of friction within the range of predefined tribological conditions.

This paper describes the application of a neural network method for modelling tribological processes in the winding-gear disc brakes and subsequently might be used for the pad material optimisation.

Brake friction material consists of dozen or more different constituents, combining organic, metallic, and ceramic phases. Their performance characteristics include the coefficient of friction, resistance to wear, stiffness, thermal conductivity, and environmental impact. The brake performance is influenced by tribological conditions between a brake disc and brake pad, characterised by sliding speed, pressure, and temperature distribution. Tribological tests were carried out with particular emphasis on accurate measurement of the friction and wear properties of the brake pair. The size of the brake disc (Fig. 1), work safety, and cost considerations concerned with any winding gear operation caused the testing to be carried out on a small scale tribotester. These tests were set up to provide a comparison between various friction materials tested against the same disc in both criteria, i. e. friction and wear [2].

In this paper, only the friction criterion (coefficient of friction) was taken into consideration, because the stability of the emergency braking is the operational priority in winding installations. The modelling and prediction of the tribological processes within disc brake by the application of the artificial neural network (ANN) method FFBP (Feed Forward Back Propagation) type consisted of relating the friction process (coefficient of friction) versus friction material formulation and testing conditions. The neural computation ability to model complex non-linear, multi-dimensional functional relationship directly from experimental data, without any prior assumption about input/output relationship, has been used in this paper.

In the course of this work, it was found that the neural network method is a powerful approach to the analysis of the experimental results and that the accuracy of prediction of tribological processes obtained by the method was significantly better than the results achieved by the multiple regression analysis [2].

Experimental method and results

Brake friction materials tested

In these tribological experiments, specially prepared samples of the brake pad materials were used. The materials are intended to work in dry conditions most of the time, even though they may be unintentionally lubricated by the rainwater or even oil. There are four main components of brake pad materials, namely, the binder, reinforcing fibres, organic and inorganic fillers, metal powders and composite premix master batch which complements mixture ratio to 100% (Table 2).

Table 2. Range of the components volume fraction [2]
Tabela 2. Objętościowy udział składników [2]

No	Component	Volume fraction, %
1	Binder (phenolic resin)	4.00 – 6.50
2	Reinforcing fibres	16.30 – 17.80
3	Fillers (inorganic and organic)	38.35 – 41.88
4	Additives (metals powders)	26.85 – 29.32
5	Composite premix master batch	7.00 – 12.00

The purpose of the binder is to maintain the brake pads structural integrity under mechanical and thermal stresses. It has to hold the components of the brake pad together [3, 4]. The choice of binders for brake pads is an important issue, because if it does not remain structurally stable at high temperature other components such as the fibres and powders will disintegrate. The purpose of reinforcing fibres is to provide mechanical strength to the brake pad. Friction materials typically use a mixture of different types of reinforcing fibres (ceramic, aramid, metallic) with complementing properties. The fillers in a brake pad are present for the purpose of improving its manufacturability. Fillers play an important role in modifying certain characteristics of brake pads, namely, noise suppression, heat stability or the friction coefficient stability. Metal powders (brass, copper and steel) have very high heat conductivities; therefore, they are able to remove heat from the friction surfaces very quickly. Premix master batch is used as a complement of a composite to 100%. All testing samples of friction material, no matter what composition (material formulation), were produced by the same manufacturing procedure defined by conditions of dry mixing and hot moulding (170°C and 90 MPa).

Range of experimental testing

The proper friction brake design requires complete information about tribological characteristics of the friction pair (pad material versus disc material) in the full range of the operational parameters, namely, pressure, and sliding speed and temperature on the friction surfaces.

Carrying out experimental tests on the industrial installations is not always possible. In some cases this, inability arises from the fact that the installation has not been built or come from the safety codes, or simply from cost consideration. The investigations on friction characteristics of the brake materials for mine hoist brake systems were made on the scaled-down inertia dynamometer (Fig. 2) [2] due to the above reasons.

The experiments were conducted in accordance with the principles of the tribological similarity developed by Sanders et. al. [5].

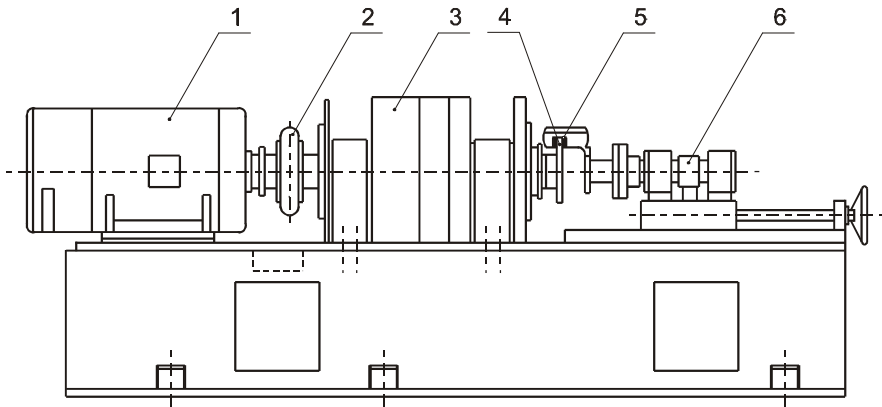


Fig. 2. Schematic diagram of scaled-down inertia dynamometer, where: 1 – electric motor, 2 – flexible coupling, 3 – flywheel, 4 – brake disc, 5 – specimens holder, 6 – torquemeter

Rys. 2. Schemat stanowiska bezwładnościowego do badań tarcia, gdzie: 1 – silnik elektryczny, 2 – sprzęgło, 3 – masa bezwładnościowa, 4 – tarcza hamulca, 5 – głowica do mocowania próbek, 6 – dźwignia pomiarowa momentu tarcia

The numerical values of input parameters for operational variables and friction materials formulations were established making use of factorial and simplex designs. Experimental sample formulations are shown in Table 3.

Friction tests were performed on the inertia disc brake dynamometer (Fig. 2) and the following set of conditions were used during testing:

1. Running – in of samples friction surface:
 - sliding speed $v = 6.5 \text{ m/s}$
 - pressure $p = 1.2 \text{ MPa}$
 - initial temperature $T = 60^\circ\text{C}$
2. Pressure test:
 - pressure $p = 1.2; 2.4; 3.6; 4.8 \text{ MPa}$

- sliding speed $v = 9.0$ m/s
 - initial temperature $T = 60^{\circ}\text{C}$
3. Sliding speed test:
- sliding speed $v = 4; 6; 8; 10; 12$ m/s
 - pressure $p = 3.0$ MPa
4. Temperature test:
- initial temperature $T = 60; 100; 140; 180; 240; 280; 320; 360^{\circ}\text{C}$
 - sliding speed $v = 9$ m/s
 - pressure $p = 3.0$ MPa
- Complete set of arithmetic mean values of the coefficient of friction is presented in Tables 4, 5 and 6.

Table 3. Samples composition
Tabela 3. Składy próbek

Ingredient	Binder, Phenolic resin	Composite premix masterbatch	Reinforcing fibres	Fillers	Additives, Metal powders
	X_1	X_2	X_3		
No sample	%				
1	6.50	7.00	17.30	40.71	28.49
2	6.50	12.00	16.30	38.35	26.85
3	4.00	7.00	17.80	41.88	29.32
4	6.50	9.50	16.80	39.53	27.67
5	5.25	12.00	16.55	38.94	27.26
6	4.00	9.50	17.30	40.71	28.49
7	5.25	9.50	17.05	40.12	28.08
8	5.67	10.33	16.80	39.53	27.67

Friction process modelling in brakes by means of neural computation

Application of Feed Forward Back Propagation (FFBP) type of ANN method

In the first step on application of FFBP type ANN analysis friction model was designed. In the model design, the experimental data presented in Tables 4 to 6 were used. The set of arithmetic mean values of the coefficient of friction was obtained for 17 combinations of the test parameters (pressure, sliding speed and temperature) and for 8 combinations of the friction materials compositions. Friction tests were conducted three times for every pair of the combinations (test parameters and materials compositions) leading to completion of the set of input data for ANN which was composed of 468 vectors.

The set of input data was divided on three equal parts: the training, the validation, and the testing data sets using suitable for the purpose software [2]. Before the neural computation, the data scaling was performed in order to reach variability range of the characteristic suitable to the neuron activation function

Table 4. Arithmetic mean values of coefficient of friction (pressure test)
Tabela 4. Średnie wartości współczynnika tarcia (próba ciśnieniowa)

Test parameter		No of sample																
v	p	1		2		3		4		5		6		7		8		
m/s	MPa	μ	T_k °C	μ	T_k °C	μ	T_k °C	μ	T_k °C	μ	T_k °C	μ	T_k °C	μ	T_k °C	μ	T_k °C	
	1.2	1	0.605	252	0.677	247	0.576	246	0.677	257	0.605	248	0.677	253	0.560	228	0.515	236
		2	0.634	248	0.677	246	0.605	241	0.677	257	0.605	248	0.662	256	0.575	230	0.515	243
		3	0.634	248	0.691	244	0.605	245	0.677	257	0.619	240	0.662	252	0.590	235	0.530	242
	2.4	1	0.583	246	0.665	247	0.575	245	0.583	241	0.568	244	0.605	248	0.590	224	0.553	233
		2	0.598	256	0.673	247	0.590	248	0.590	246	0.575	244	0.612	248	0.605	232	0.553	247
		3	0.598	264	0.658	247	0.590	254	0.598	245	0.590	250	0.605	247	0.613	228	0.560	241
9	3.6	1	0.560	248	0.611	234	0.555	244	0.565	239	0.550	236	0.580	236	0.580	229	0.554	232
		2	0.575	256	0.611	238	0.570	251	0.580	249	0.560	240	0.590	242	0.590	232	0.570	241
		3	0.575	253	0.616	242	0.575	240	0.580	245	0.575	247	0.585	235	0.590	232	0.570	239
	4.8	1	0.545	246	0.583	230	0.545	230	0.541	237	0.545	238	0.556	226	0.553	230	0.530	241
		2	0.553	256	0.587	234	0.553	242	0.549	237	0.556	230	0.564	229	0.556	230	0.552	242
		3	0.560	256	0.583	231	0.556	237	0.556	243	0.556	230	0.572	223	0.560	234	0.560	243

Table 5. Arithmetic mean values of coefficient of friction (speed test)
 Tabela 5. Średnie wartości współczynnika tarcia (próba prędkościowa)

Test parameter	v m/s	p MPa	No	No of sample															
				1		2		3		4		5		6		7		8	
				μ	T_k °C	μ	T_k °C	μ	T_k °C	μ	T_k °C	μ	T_k °C	μ	T_k °C	μ	T_k °C	μ	T_k °C
			1	0.614	98	0.698	98	0.644	99	0.620	96	0.656	94	0.674	100	0.608	97	0.584	98
	4		2	0.620	100	0.674	95	0.650	99	0.638	101	0.662	98	0.666	94	0.626	98	0.614	98
			3	0.632	98	0.674	98	0.668	97	0.637	95	0.680	95	0.666	96	0.626	97	0.614	96
			1	0.620	154	0.626	150	0.638	146	0.608	140	0.632	148	0.644	143	0.632	140	0.608	142
	6		2	0.638	154	0.626	150	0.650	133	0.638	138	0.650	148	0.643	143	0.656	142	0.626	144
			3	0.644	154	0.656	160	0.650	133	0.625	142	0.632	148	0.656	141	0.662	142	0.626	144
			1	0.614	226	0.602	219	0.608	207	0.590	210	0.590	216	0.614	202	0.620	191	0.596	212
	8	3	2	0.614	216	0.620	219	0.608	205	0.602	214	0.602	216	0.614	202	0.626	194	0.608	206
			3	0.614	217	0.620	214	0.584	204	0.596	205	0.602	215	0.626	200	0.620	196	0.596	200
			1	0.578	306	0.596	302	0.561	301	0.573	291	0.566	291	0.596	286	0.590	264	0.572	288
	10		2	0.590	296	0.602	310	0.572	302	0.584	280	0.572	292	0.596	293	0.590	270	0.578	275
			3	0.596	314	0.602	312	0.578	299	0.579	282	0.572	298	0.579	285	0.584	276	0.578	275
			1	0.531	395	0.566	367	0.531	376	0.544	368	0.537	396	0.561	385	0.507	374	0.507	381
	12		2	0.566	380	0.572	368	0.549	364	0.567	360	0.543	396	0.566	373	0.525	377	0.537	384
			3	0.561	390	0.561	359	0.531	374	0.561	365	0.531	416	0.555	376	0.525	372	0.522	383

Table 6. Arithmetic mean values of coefficient of friction (temperature test)
Tabela 6. Średnie wartości współczynnika tarcia (proba temperaturowa)

Test parameter		No of sample																
		1		2		3		4		5		6		7		8		
v	p	T_p	μ	T_k	μ													
m/s	MPa	°C		°C		°C		°C		°C		°C		°C		°C		
		60	0.579	224	0.566	223	0.549	223	0.525	228	0.555	218	0.566	217	0.543	222	0.513	238
			0.576	227	0.584	228	0.566	223	0.543	234	0.566	212	0.572	229	0.561	234	0.543	238
			0.578	234	0.584	231	0.566	224	0.555	232	0.572	214	0.578	232	0.555	234	0.549	236
		100	0.584	276	0.574	261	0.561	273	0.549	263	0.564	268	0.566	260	0.555	272	0.555	282
			0.584	283	0.572	258	0.561	272	0.561	262	0.561	270	0.572	257	0.555	285	0.555	282
			0.572	283	0.575	266	0.549	271	0.561	262	0.563	274	0.566	266	0.549	276	0.549	278
		140	0.555	313	0.561	295	0.533	309	0.549	299	0.549	314	0.556	292	0.525	318	0.531	318
			0.549	311	0.566	299	0.531	305	0.555	295	0.537	316	0.554	294	0.519	322	0.525	324
			0.549	308	0.566	301	0.532	319	0.549	296	0.537	312	0.555	297	0.519	314	0.525	316
		180	0.537	342	0.555	327	0.513	350	0.543	330	0.513	356	0.537	337	0.489	349	0.501	366
			0.537	342	0.561	336	0.519	344	0.537	339	0.519	350	0.543	333	0.495	364	0.513	366
			0.531	342	0.561	324	0.525	352	0.543	339	0.519	350	0.543	331	0.513	362	0.519	366
		240	0.525	370	0.543	357	0.507	378	0.525	370	0.507	381	0.525	370	0.507	396	0.483	416
			0.525	376	0.549	368	0.519	389	0.531	373	0.519	384	0.543	377	0.501	396	0.513	420
			0.531	382	0.566	368	0.519	396	0.537	373	0.519	383	0.549	367	0.513	400	0.519	407
		280	0.513	409	0.537	396	0.495	409	0.513	406	0.495	410	0.507	412	0.489	440	0.459	454
			0.531	400	0.549	411	0.489	405	0.519	406	0.519	415	0.531	404	0.483	440	0.477	462
			0.525	406	0.561	398	0.514	409	0.531	397	0.519	408	0.531	403	0.495	440	0.501	443
		320	0.477	434	0.513	423	0.447	469	0.479	434	0.459	438	0.471	436	0.400	474	0.429	473
			0.501	438	0.495	437	0.483	464	0.477	436	0.471	443	0.477	455	0.447	462	0.417	487
			0.513	429	0.501	437	0.489	448	0.478	443	0.483	443	0.483	445	0.435	466	0.429	482
		360	0.429	474	0.483	475	0.447	464	0.453	470	0.429	453	0.471	471	0.394	496	0.405	509
			0.465	475	0.471	471	0.433	478	0.447	471	0.453	466	0.465	475	0.411	493	0.400	516
			0.459	473	0.465	471	0.447	471	0.447	463	0.447	470	0.465	475	0.417	514	0.405	513

(mini-max function). In the case of input data x_{in} , the scaling range was from 0.1 to 1.0 (Equation 1) and for output data the scaling range was from 0.1 to 0.9 (Equation 2).

$$x_{in} = \frac{X - X_{min}}{X_{max} - X_{min}} \cdot 0.9 + 0.1 \quad (1)$$

$$x_{out} = \frac{X - X_{min}}{X_{max} - X_{min}} \cdot 0.8 + 0.1 \quad (2)$$

ANN design process includes value evaluation of coefficient of training η , which is inherent to the sorted out problem. The design process also covers the test stage recognition in which training can be considered as completed. The completion of the ANN's training can be determined by analysis of the root-mean-square value of error, E and the maximum error E_{max} (Equations 3 and 4).

$$E = \sqrt{\frac{1}{p} \sum_{j=1}^p (z^j - y^{j(L)})^2} \quad (3)$$

$$E_{max} = \max \{abs(z^j - y^{j(L)})\} \quad (4)$$

where:

- p – number of vectors,
- L – output layer index,
- z^j – expected value in the network output,
- z – mean value from z^j ,
- $y^{j(L)}$ – neuron answer in output layer.

In addition, the efficiency of the ANN training action can be represented by the coefficient of determination, B (Equation 5).

$$B = \frac{\sum_{j=1}^p (z^j - y^{j(L)})^2}{\sum_{j=1}^p (y^{j(L)} - z)^2} \quad (5)$$

The coefficient of determination B reflects the degree of accuracy in representations between the investigated process and the model. The closer the

coefficient of determination to unity ($B \rightarrow 1$), the better is the representation of the expected values by the values generated by the model.

The architecture of the network FFBP type consists of three layers (Fig. 3), namely, the input layer, the hidden layer, and the output layer.

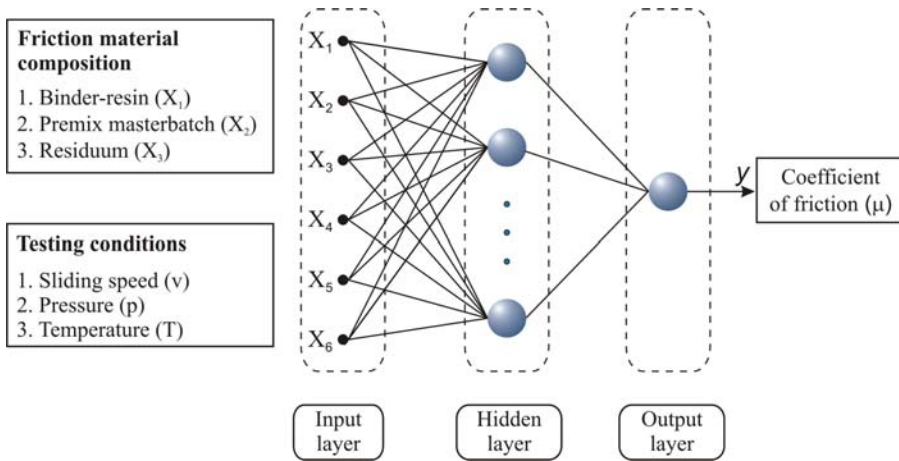


Fig. 3. Structure of the ANN type FFBP used for friction modelling process

Rys. 3. Budowa sieci neuronowej typu FFBP wykorzystanej do modelowania procesów tarcia

During the training process, the values of the coefficient of friction were observed from output as the result of input parameter insertion into the network (Table 7).

Table 7. Input and output vectors in network FFBP type for friction model
Tabela 7. Wektory wejściowe i wyjście sieci typu FFBP dla modelu tarcia

Input vectors						Output vector
Materials parameters			Friction parameters			Friction coefficient
1	2	3	4	5	6	7
X_1	X_2	X_3	v	p	T	μ

Preliminary analysis shows that optimal value of the coefficient of training is $\eta = 0.06$, which was achieved as a compromise between the accuracy and swiftness of the training process.

Fixing a number of neurons in the hidden layer was undertaken in the next step of building up the architecture of a network.

FFBP type ANNs are able to represent any functional relationship between input and output, if there are enough neurons in the hidden layer [6]. However,

too many neurons in the hidden layer may cause “over fitting”. The optimal is to use a network that is just large enough to provide an adequate fit. In order to reach the optimal solution, training was performed with arbitrarily selected number of 20 neurons in the hidden layer, and subsequently the training procedure was repeated several times with one neuron less in the hidden layer. Results from these tests, including calculated values of the root-mean-square error, E and the maximum error, E_{\max} , are presented on Figure 4.

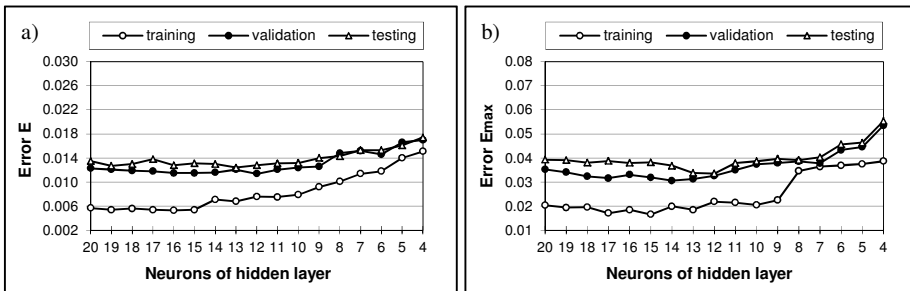


Fig. 4. Number of neurons in the hidden layer effect on error: a) E , b) E_{\max}

Rys. 4. Wpływ kolejno usuwanych neuronów warstwy ukrytej na wartość błęd: a) E , b) E_{\max}

An increase in both errors E and E_{\max} was noticed below 12 neurons in the hidden layer; therefore, the structure of network 6-12-1 was recommended for modelling friction process in the disc brake.

Determination of the friction conditions and the composition of friction materials effect on the coefficient of friction

An attempt was made to determine magnitude of the effect by friction parameters (v , p , T) and materials parameters (X_1 , X_2 , X_3) on the coefficient of friction. The magnitude of effect determination is based on the selecting method of the input feature for ANN [7]. The method is called “weight pruning”.

In the method assumption is that the significance of the inputs to the network is equivalent to the magnitude of the effect made by the parameter on the analysed process.

The results of the weight pruning process in the form of the significance level for all input parameters are presented in Figure 5.

All input parameters to the network (Table 7) have a significance level above 70%. The results indicate that friction parameters (v , p , T) and material parameters (X_1 , X_2 , X_3) taken into consideration in the experimental part have a high and equivalent effect on coefficient of friction. The results confirm the friction model correctness.

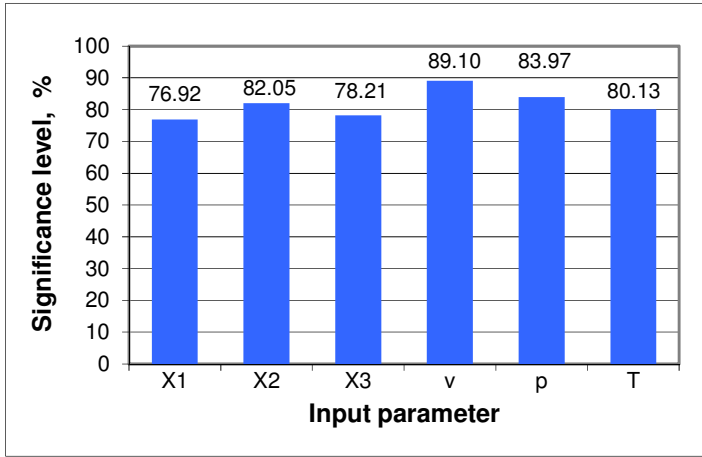


Fig. 5. Significance level for input parameters to the network
 Rys. 5. Istotność parametrów wejściowych sieci

In the next step of ANN modelling evaluation, the comparative analysis was made between the quality of several models, namely, the model developed by neural network with structure 6-12-1 (Figure 3) and models obtained by multiply regression analysis (MRA) (Table 8). Errors E and E_{max} for neural network friction model are 2 to 5 times lower than MRA models, which clearly indicates the higher quality of ANN type FFBP modelling of friction process. The same conclusion can be made analysing values of the coefficient of determination B (Figure 6).

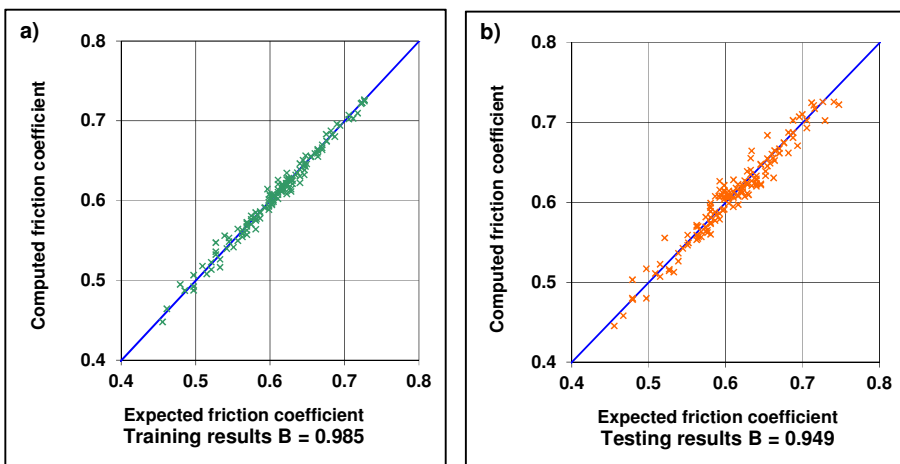


Fig. 6. Comparison between expected and computed results, for:
 a) training data set, b) testing data set

Rys. 6. Porównanie wyników oczekiwanych i obliczonych dla: a) zbioru trenującego, b) zbioru testującego

Table 8. Results of the comparison between several friction models
Tabela 8. Wyniki dla modeli procesu tarcia

No	Model name	Training results			Testing results		
		E	E _{max}	B	E	E _{max}	B
	1	2	3	4	5	6	7
1	MRA-Linear	0.024	0.097	0.799	0.025	0.116	0.781
2	MRA-Logarithmic	0.024	0.104	0.785	0.026	0.123	0.759
3	MRA-Polynomial	0.021	0.096	0.845	0.023	0.094	0.813
4	MRA-Piecewise	0.020	0.058	0.860	0.021	0.070	0.848
5	Neural Network	0.007	0.020	0.985	0.013	0.034	0.949

High conformity between values of the coefficient of friction obtained (Figures 7 to 9) from the model and expected values confirm the purposefulness of the ANN type FFBP application for modelling friction and other tribological processes in friction brakes.

$$v = 9 \text{ m/s}; p = 3 \text{ MPa}$$

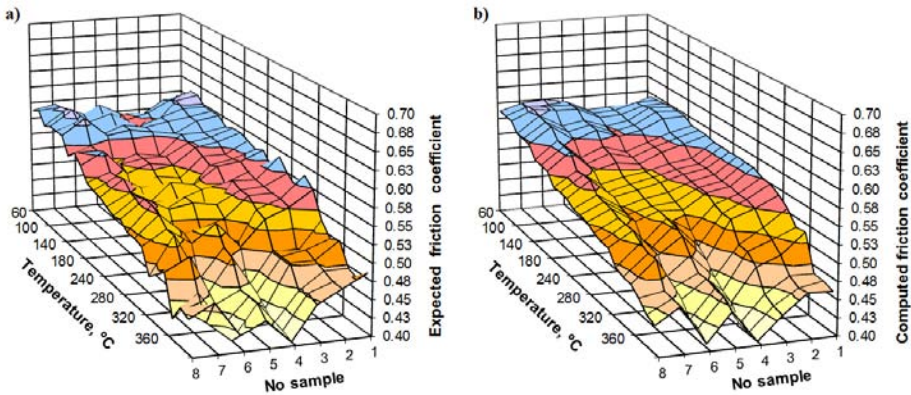


Fig. 7. Values of coefficient of friction as a function of temperature, obtained from:
a) experimental data, b) network responses

Rys. 7. Wartości współczynnika tarcia w funkcji temperatury, uzyskane z:
a) wyników badań, b) odpowiedzi sieci

$T = 60^{\circ}\text{C}; p = 3\text{MPa}$

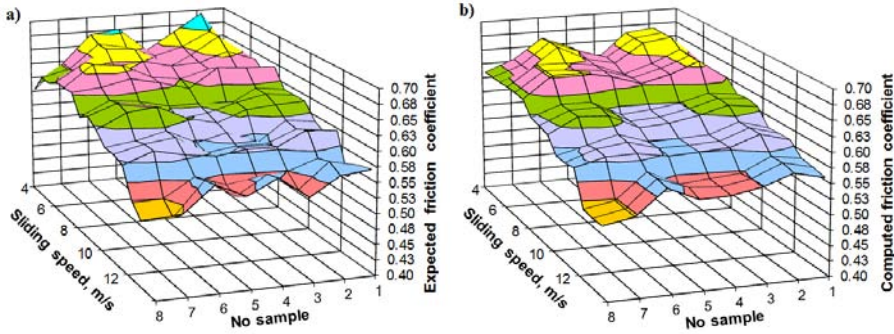


Fig. 8. Values of coefficient of friction as a function of sliding velocity, obtained from: a) experimental data, b) network responses

Rys. 8. Wartości współczynnika tarcia w funkcji prędkości poślizgu, uzyskane z: a) wyników badań, b) odpowiedzi sieci

$T = 60^{\circ}\text{C}; v = 9\text{m/s}$

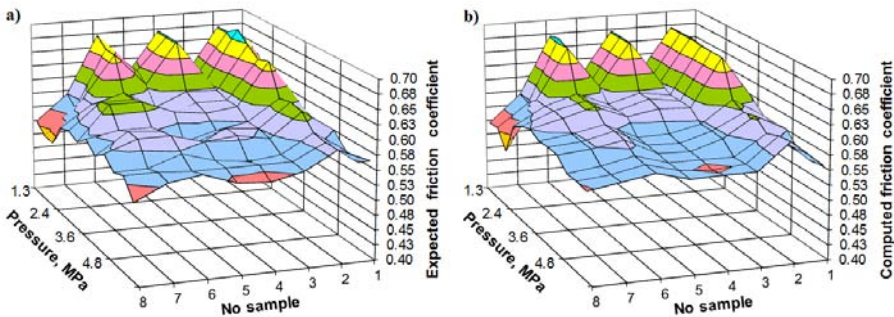


Fig. 9. Values of coefficient of friction as a function of pressure, obtained from: a) experimental data, b) network responses

Rys. 9. Wartości współczynnika tarcia w funkcji nacisku, uzyskane z: a) wyników badań, b) odpowiedzi sieci

Concluding remarks

In the course of the work, it was found that the neural network method is a powerful approach to the analysis of the experimental results and that the accuracy of the prediction of friction processes in disc brakes obtained by the ANN type FFBP method were significantly better than the results achieved by the multiply regression analysis, (MRA).

References

- [1] Ścieszka S.F.: Friction Brakes. Gliwice – Radom: ITeE; 1998.
- [2] Grzegorzek W.: Modelling tribological processes in winding gear disc brakes by mean of a neural network method. PhD thesis (in polish). Gliwice: SUT; 2003.
- [3] Chan D., Stachowiak G.W.: Review of automotive brake friction materials. J. Automobile Engineering. 2004; 218: 953–966.
- [4] Blau P.: Compositions, functions and testing of friction brake materials and their additives. Technical Report Oak Ridge National Laboratory/TM – 2001.
- [5] Sanders P.G., Dalka T.M., Bash R.H.: A reduced – scale brake dynamometer for friction characterization. Tribology International. 2001; 34: 609–615.
- [6] Aleksendric D., Duboka C.: Automotive friction material development by means of neural computation, Conference Proceedings “Braking 2006”, York: 2006; 167–176.
- [7] Sokołowski A.: Neural network application for tool point condition monitoring. PhD thesis (in polish). Gliwice: SUT; 1994.

Prognozowanie charakterystyk ciernych hamulców maszyn wyciągowych z zastosowaniem sztucznych sieci neuronowych

Streszczenie

Bezpieczeństwo i niezawodność działania to główne wymagania stawiane hamulcom maszyn wyciągowych. Niezawodna, bezproblemowa praca hamulców w zmieniających się warunkach otoczenia i obciążenia jest wymagana i egzekwowana przez dozór górniczy. Dlatego wybór materiałów na elementy pary hamulcowej (okładzina cierna, tarcza hamulca) jest dużym wyzwaniem dla konstruktorów. Współczynnik tarcia dla tej pary ciernej powinien być względnie wysoki (około 0,4), ale przede wszystkim wymaga się, aby był stabilny. Dla osiągnięcia pożądanego efektu pracy hamulca zastosowano nowe narzędzie dla predykcji i kontroli procesów tribologicznych w funkcji parametrów tarcia i składu chemicznego materiału okładziny hamulcowej. Zastosowanie sztucznych sieci neuronowych jest przydatne w modelowaniu złożonych, wieloczynnikowych zależności w oparciu o dane pochodzące z eksperymentów laboratoryjnych. Sztuczne sieci neuronowe mogą być wytrenowane do wytworzenia relacji wejście/wyjście i do modelowania oraz przewidywania charakterystyk użytkowych w hamulcach ciernych.